JOURNAL OF NANO- AND ELECTRONIC PHYSICS
Vol. **7** No 3, 03008(6pp) (2015)

ЖУРНАЛ НАНО- ТА ЕЛЕКТРОННОЇ ФІЗИКИ
Том **7** № 3, 03008(6cc) (2015)

The Impact of Cracked Microparticles on the Mechanical and the Fracture Behavior of Particulate Composite

Waleed K. Ahmed[1,*], Wail N. Al-Rifaie[2,†]

[1] *United Arab Emirates University, Faculty of Engineering, ERU, Al Ain 15551, UAE*
[2] *Civil Engineering Department, Philadelphia University, Amman, Jordan*

(Received 02 May 2015; published online 20 October 2015)

In this investigation a metallic composite with a cracked micro has been investigated using finite element method. Particulate reinforced composite is one of the most favorite composite due to it quit isotopic properties. While being in metallic status, the micro particles may be subjected to deterioration which lead to crack embedded initiation within the micro particle. This crack lead to degradation in the mechanical as well as the fracture behavior in the composite. Mechanical characteristics through estimating the stiffness of the composite has been studied for intact and cracked particles as well as for the fractured particles. It has been found that as long as the crack propagates in the micro particle, there is reduction in the composite stiffness and increases in the stress intensity factor (SIF).

Keywords: Composite, FEM, Fracture, Mechanical properties, Particles, SIF.

PACS numbers: 02.70. – c, 46.50. + a, 81.05.Qk, 81.07.b, 83.10.Rs

1. INTRODUCTION

In order to improve the characteristics of a material, by introducing a second phase, either in the form of fibers or particulates is the traditional way implemented to improve the properties of a material. Over the past decades, many composites have been developed by mixing a micro-sized to the matrix as reinforcements. At the present time, the main interest has been focused on nanocomposites, i.e., materials in which the secondary phase is nano-sized. Moreover, the characterization and failure of the composite still the main concern of the researches, therefore a massive attention has been spent to elucidate the factors affect the failure and hence the deterioration of the composite stiffness, especially in term of fracture mechanics.

The self-organization of the set of active nanoparticles was analyzed on the basis of phase portraits [1], whereas $Cd_xZn_{1-x}S$ nanoparticles have been synthesized using hydrothermal method. Structural characterization was done by XRD where the lattice structure gradually changes from hexagonal to cubic with increasing percentage of Zn in$Cd_xZn_{1-x}S$ nanoparticles [2]. It was reported that the comparison between ZnO nanoparticles prepared via two different routes. It was found that when prepared under the same ambient conditions viz temperature, pressure etc. and keeping all the parameters same, the nanoparticles prepared via Sol-gel route were highly crystalline and had smaller crystallite size as compared to the one prepared by Solid state reaction method [3]. On the rother hand, $Zn_{1-x}Mn_xS$ nanoparticles were synthesized using a co-precipitation method. Structural characterization by X-Ray diffraction (XRD) measurement revealed that all the synthesized samples were crystallize in the monophasic cubic zinc blende structure and monotonous decrement in the lattice constants with increasing Mn content, due to the effective Mn doping [4]. The Cu_2ZnSnS_4 (CZTS) nanoparticles were successfully synthesized by Chemical co-precipitation method with different synthesis temperatures. The synthesized nanoparticles were characterized by X-ray diffraction, Raman Spectroscopy, Scanning electron microscopy, Energy dispersive spectroscopy and UV-VIS-NIR spectrophotometer [5]. Metal-carbon nanocomposites on the basis of polyacrylonitrile and compounds of metals (Fe, Ni, Co) synthesized at IR-heating and studied by SEM, X-ray phase analysis, Raman scattering, IR Fourier spectroscopy are characterized by the carbon nanostructured amorphous graphite matrix with uniformly distributed nanoparticles of metals (10-30 nm), their oxides and compounds – $FeNi_3$ and FeCo, multilayered carbon nanotubes (~ 7-22 nm), and in the composition of Fe-Co / C fullerene-like formations – C_{60} [6]. While efforts have been made to synthesize quaternary alloy nanostructures with high surface area for application in many fields, a detailed exploration of quinternary alloy nanostructures has not been reported until now. This work investigates the optimum crystallization parameters for reducing crystal defects in $Cu_2Zn_{1-x}Cd_xSnS_4$ quinternary alloy nanostructures [7]

Particle fracture is one of the fundamental damage mechanisms of particle-reinforced composite materials, therefore Mehmet et al. [8] and many researchers demonstrated that the fracture behavior of sand particles in DEM using agglomerates showed that it is quite match the 3D physical shape of silica sand particles by mapping the 3D particle morphology from the SMT images. It was explained that agglomerates that closely match the physical shape of sand particles which can better reproduce the mode of failure, orientation of particles, and contact configuration when compared to spherical agglomerates. Ceramic and silica particles can effectively reinforce bulk polymers [9], whereas an oxide ceramic based composite of Al_2O_3-SiO_2-ZrO_2 (ASZ) sys-

* w.ahmed@uaeu.ac.ae
† wnrifaie@yahoo.com

tem was developed and investigated using a pressureless sintering route [10]. The effect of compositions of each component on the microstructure, i.e., density and hardness properties were studied. Gurusamy and Prabu [11] demonstrated the results of a study carried out to understand the effect of the squeeze pressure on the mechanical properties of Al / SiCp composites, fabricated by the squeeze casting. A numerical studies intensively used, which are mainly based on the finite element technique for the optimization of mechanical properties by changing of intrinsic parameters. The depreciation in body stiffness results from the existence of fractured particles. Therefore, it becomes important to predict the stiffness change of particulate composites as a function of the extent of particle fracture, particularly from the view point of damage-tolerant design of composite structures [12]. It was predicted the effective Young's modulus of a particulate composite containing fractured particles by considering some particles were fractured while others remained intact. Many studies were done on particulate composites with particle fracture. A double-inclusion model, originally developed to determine effective linear elastic properties of composite materials, was reformulated and extended to predict the effective nonlinearelastic-plastic response of two-phase particulate composites reinforced with spherical particles [13]. FEM was used to predict the impact of a precrack on the mecjsnicsl properties of fiber reinforced polymer [14]. Basically, the first principle work of Mori and Tanaka [15], originally concerned with calculating the average internal stress in the matrix of a material containing precipitates with eigenstrains. The method is to estimate the average internal stress in the matrix of a material containing inclusions with transformation strain. The Mori-Tanaka method was extended to determine the effective Young's modulus of the composite weakened by the fractured particles, where the case falls within the general subject of stiffness properties of cracked solid materials [16]. A reformulation of the Mori-Tanaka's theory in its application to the computation of the effective properties of composites was adopted by Benveniste [17]. Moreover, finite element method (FEM) was adopted for comparison. Based on the incremental damage theory, the influences of particle-cracking damage and its residue strengthening capacity on the stress-strain response of particle reinforced (metal matrix composite) MMC under uniaxial tension were investigated by Jiang et al. [18]. Different damage modes were identified for particle reinforced metal matrix composite (PMMC) [19]. It was reported that for a certain PMMC under the specific loading, the corresponding damages mainly rely on the constituent's properties, the interface bonding, particle shape and distribution in the matrix [20]. Among these damage modes, particle-cracking is regarded as a very serious case that badly decreasing the strength, ductility and fracture toughness of PMMC. A thorough understanding of dependence of particle cracking on the microstructures is thus essential. Many researchers have been reported about damage-structure relationship that carried out by different methods. Maire et al. [21] proposed a model which incorporated damage, where the model treats damaged and undamaged regions as distinct continuous phases and allows the relative volume fraction of each phase to vary during deformation. Besides the model considers the influence of particle size and incorporates the results of existing Finite Element Method (FEM) calculations. Ahmed [22] investigated the impact of the interfacial debonding on the mechanical properties of nanofiber reinforced composites. Godoy et al. [23] identified the stress redistributions that take place at the unit cell level, in which damage has already occurred due to an independent process. Damage is modelled by means of interface defects, in which the number and size of defects are considered as parameters of the damaged configuration and also by changes in material properties. RSA (Random Sequential Adsorption) method was used [24] to generate the representative volume element RVE models of syntactic foams particulate composites made of syntactic foams obtained by filling a polymeric matrix with hollow glass microballons (HGMs). Besides, through the finite element analysis based on RVE models, it was obtained effective elastic constant of syntactic foams and microscopic stress field distribution. It was found that wall-thickness ratio of HGM plays a crucial role in the effective Young's modulus. A spherically shaped filler diameter and interphase effects on the Young's modulus of micro and nano size silicon dioxide (SiO_2) particle reinforced epoxy composite materials were investigated by Jang et al. [25]. Both micro- and nano-composites are prepared at two different particle loading fractions for tensile testing. It is observed that the nano-composites show significant increase in Young's modulus over microcomposites, showing a linear increase as particle volume fraction increases. Lin et al. [26] proposed a finite element formulation for a non-local particle method for elasticity and fracture analysis of 2D solids. The model is based on a new particle method which incorporates a non-local multi-body particle interaction into the conventional pair-wise particle interactions. The non-local particle method is capable of modeling solids with arbitrary Poisson's ratio. Finite element method was used as well to study the impact of the mismatch on the stress distribution [27]. Hua and Gu [28] predicted the thermo-mechanical behavior of 2080 aluminum alloy reinforced with SiC particles using the Mori-Tanaka theory combined with the finite element method. The influences of particle volume fraction, stiffness, aspect ratio and orientation were examined in terms of effective Young's modulus, Poisson's ratio and coefficient of thermal expansion (CTE) of the composite. For certain particle-reinforced composites, the elastic moduli measured ultrasonically did not obey the OOFEM. The mismatch was attributed to the presence of damage because of debonding between Ni and Alumina phases [29]. Recently, Kumar and Ghosh [30] studied the dynamic fragmentation of brittle materials using the cracking particles method (CPM) with obscuration zone, where the CPM is an effective meshfree method for arbitrary evolving cracks. The influence of the variation in material properties with different stochastic input parameters on the results is studied as well.

Basically, the objective of the present study is to estimate the effective stiffness for intact particles embedded in composite, and for a fully fractured particles as well. Besides, whereas fracture mechanics is used to predict stress intensity factor for a rang of the crack length.

2. PROPERTIES OF PARTICLE AND COMPOSITE

The mechanical properties of the matrix are taken to be of 200 GPa for the modulus of elasticity (E_m) and 0.38 for the Poisson's ratio (ν_m). Besides, the mechanical properties of the reinforced particle to be a Poisson's ration of $\nu_p = 0.2$, whereas a range of the modulus of elasticity of $E_p = 1000$, 2000 and 4000 GPa, which is corresponding to the particle-matrix ration (i.e., E_p/E_m) of 5, 10 and 20. Linear elastic behaviour of the particulate composite material is considered in the study, for both matrix and the reinforcement. Moreover, a perfect bonding between the particle and the matrix boundary is maintained.

3. MODELING USING FINITE ELEMENT METHOD

Finite element analysis is adopted to predict the stiffness variation of a particulate composite for intact and a fractured particles, where the fractured particle presumed to contain penny-shaped crack that divides the particle into equal halves, (i.e., the crack faces are normal to of the principal direction of the composite), as illustrated in Fig. 1.

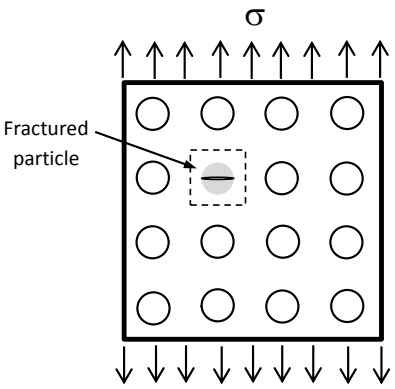

Fig. 1 – Particulate reinforced composite contains with fractured particles

Two dimensional, plane strain model is proposed to estimate the effectiveness stiffness as well as the stress intensity factor. A representative volume element (RVE) is selected for analysis, as shown in Fig. 2.

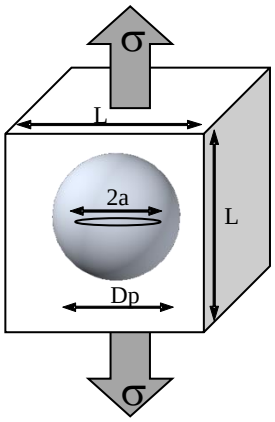

Fig. 2 – RVE for fractured particle

Due to symmetry of the RVE designated, a quarter of the studied RVE are modelled, as elucidated in Fig. 3, which represents the boundary conditions used in the FEA.

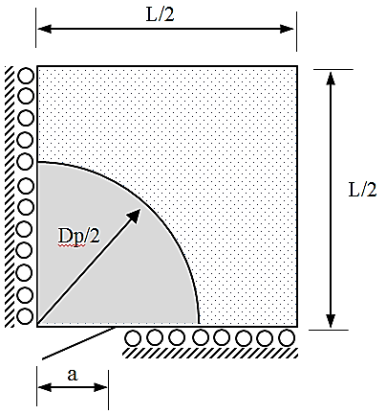

Fig. 3 – Boundary conditions for a fractured particle

Two dimensional finite element options are adopted through ANSYS software, where tt was demonstrated that 2D can be used for accepted margin of error instead of 3D analysis [31]. Basically, 8-node solid element (Plane 82) is chosen to be the candidate element to be used in the analysis. Figure 4 illustrates FE mesh of the RVE that adopted in the present analysis, where it is obvious shown the singularity elements around the crack tip.

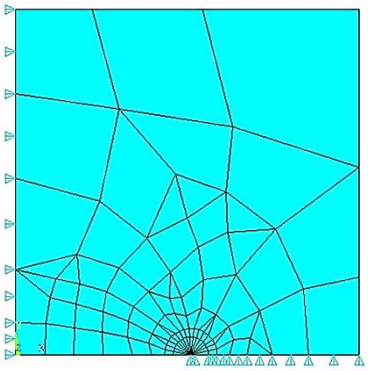

Fig. 4 – FE mesh and boundary conditions of RVE

The particle volume fraction (C_p) is considered as 0.1, 0.2, 0.3, 0.4, 0.5 and 0.6 to predict the effective stiffness of the composite, whereas for the basic reference case ($C_p = 0$ and $E = E_m$), where there is no reinforcement in the composite. In particular, the results of the effective modulus of elasticity of the composite structure was exactly identical to the matrix stiffness, i.e., E_m, which is used to verify the validity of the proposed model. Basically, plane strain conditions is applied for this verification. The composite is subjected to a unit tensile stress perpendicular on the fractured particle face. Moreover, multiple point constraint (MPC) is adopted in the analysis to maintain a uniform axial displacement of the model and hence to be applicable using Hook's principle for the stiffness estimation [32].

4. ESTIMATING COMPOSITE

Many researches have been involved in prediction of the effective Young's modulus of a particulate composites with fractured particles and even with highly approximate analytical solutions, FEM [33]. As a matter of fact, it is known that estimation the effective stiffness of the composite is considered relatively quit easy of a periodic particle arrangement packing [34]. This allows adopting a repeated unit cell with a periodic boundary conditions, so eventually the determination of the target properties is an easy job. However, it is an important matter to predict the variation in the stiffness of a composite material with deteriorated particles, since the final stage of the failure depend essentially on the reinforcement properties. Using an extension to Mori-Tanaka method to determine the effective Young's modulus of fractured particles composite materials was done by Teng [12] with detailed derivations, where the average stress and strain of a single fractured particle within an infinite matrix and subjected to a remote stress. A verification of the extended method was accomplished using 3D finite element method, which revealed an excellent agreement with the developed model of a particle composite with body-centred cubic packing as well as with the available experimental results. The main objective of the study is to estimate the effective Young's modulus, i.e., stiffness, of the particulate composite material through two scenarios, fully intact and fractured particles. Due to complications of the 3D FEA, especially whenever involves fracture mechanics prediction, usually researchers simplify the studied cases into 2D analysis and accepting minor errors due to approximations adopted. Mainly this technique is a popular and widely used especially taking into account the time and efforts spent in the modelling as well as the execution time of the FE models.

The effective Young's modulus is predicted through a simplified principle of solid mechanics, i.e., Hook's law [32]. The generalized Hooke's Law in 3D assumes that the material is elastic and isotropic, strain-to-stress relations can be expresses as:

$$\begin{bmatrix}\epsilon_{xx}\\ \epsilon_{yy}\\ \epsilon_{zz}\\ \gamma_{xy}\\ \gamma_{yz}\\ \gamma_{zx}\end{bmatrix}=\begin{bmatrix}\frac{1}{E} & -\frac{\upsilon}{E} & -\frac{\upsilon}{E} & 0 & 0 & 0\\ -\frac{\upsilon}{E} & \frac{1}{E} & -\frac{\upsilon}{E} & 0 & 0 & 0\\ -\frac{\upsilon}{E} & -\frac{\upsilon}{E} & \frac{1}{E} & 0 & 0 & 0\\ 0 & 0 & 0 & \frac{1}{G} & 0 & 0\\ 0 & 0 & 0 & 0 & \frac{1}{G} & 0\\ 0 & 0 & 0 & 0 & 0 & \frac{1}{G}\end{bmatrix}\begin{bmatrix}\sigma_{xx}\\ \sigma_{yy}\\ \sigma_{zz}\\ \tau_{xy}\\ \tau_{yz}\\ \tau_{zx}\end{bmatrix}+\alpha\Delta T\begin{bmatrix}1\\1\\1\\0\\0\\0\end{bmatrix} \quad (1)$$

where:

σ_{ii} is normal stress in ii direction, Pa
τ_{ij} is shear stress in ij direction, Pa
ϵ_{ii} is normal strain in ii direction
γ_{ij} is shear strain in ij direction
E is modulus of elasticity, Pa
G is modulus of rigidity, Pa
T is temperature
α is coefficient of thermal expansion
ν is Poisson's ratio

To get stresses if the strains are given, the most expedient method is to invert the matrix equation:

$$\begin{bmatrix}\sigma_{xx}\\ \sigma_{yy}\\ \sigma_{zz}\\ \tau_{xy}\\ \tau_{yz}\\ \tau_{zx}\end{bmatrix}=\begin{bmatrix}\hat{E}(1-\nu) & \hat{E}\nu & \hat{E}\nu & 0 & 0 & 0\\ \hat{E}\nu & \hat{E}(1-\nu) & \hat{E}\nu & 0 & 0 & 0\\ \hat{E}\nu & \hat{E}\nu & \hat{E}(1-\nu) & 0 & 0 & 0\\ 0 & 0 & 0 & G & 0 & 0\\ 0 & 0 & 0 & 0 & G & 0\\ 0 & 0 & 0 & 0 & 0 & G\end{bmatrix}\begin{bmatrix}\epsilon_{xx}\\ \epsilon_{yy}\\ \epsilon_{zz}\\ \gamma_{xy}\\ \gamma_{yz}\\ \gamma_{zx}\end{bmatrix}-\frac{E\alpha\Delta T}{1-2\upsilon} \quad (2)$$

Here is an "effective" modulus modified by Poisson's ratio:

$$\hat{E}=\frac{E}{(1-2\upsilon)(1+\upsilon)} \quad (3)$$

For uniaxial deformation, and by neglecting the thermal effect, the stiffness of a body subjected to uniaxial stress can be estimated via Hook's principle, which is represented by:

$$E=\frac{\sigma}{\varepsilon} \quad (4)$$

where:

E is Young's modulus (i.e., stiffness), Pa
σ is the applied stress, Pa
ε is strain

Accordingly, the effective stiffness of the particulate composite subjected to uniaxial stress was calculated through the following equations:

$$E_{effective}=\frac{\sigma.L}{U_x} \quad (5)$$

where:

L is the length of the RVE (i.e., the quarter model of the particulate composite)
U_x is the FE result of axial displacement corresponding to the applied stress σ.

In this regard, it is important to clarify that MPC (multiple point constraint) is adopted in the analysis on the edge where the uniaxial stress is applied to maintain a uniform axial displacement of the model and hence to be applicable using Hook's principle.

5. RESULTS AND DISCUSSION

The first phase of the investigation is to study the impact of the deteriorated particle on the effective stiffness of the composite, where a couple of cases analyzed, intact particle as well as fully cracked particle. Basically, a multiple point constraint method (MPC) technique is used for the entire analysis for the stiffness estimation particularly. Hook's principle is used to estimate the effective stiffness of the reinforced composite for the intact case, which is based on using the displacement results. Figure 5 shows the axial displacement of the RVE of the studied particulate composite.

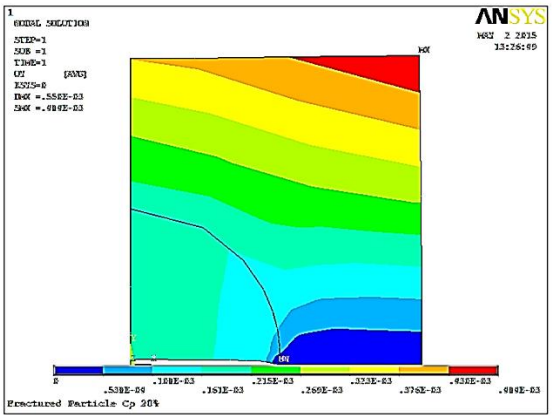

Fig. 5 – Axial displacement of the RVE contains fractured particle

It is clearly depicted from Fig. 6 that for intact particle, the effective stiffness of the composite significantly increases with the increase of the Young's modulus of the particle (i.e., E_p/E_m). Especially, it is more significant once the particle volume fraction becomes higher (i.e., $C_p > 0.1$). For intact case with $E_p/E_m = 5$, an increase in the stiffness from 1.25 up to 2.65 observed when C_p changes from 0.1 to 0.6 respectively, and this is ascribed to the particle's stiffness. In the other hand, a reduction in the stiffness observed due to presence of the crack is equal to 18 % for $C_p = 0.1$ and 79 % for $C_p = 0.6$, where the composite started losing its strength.

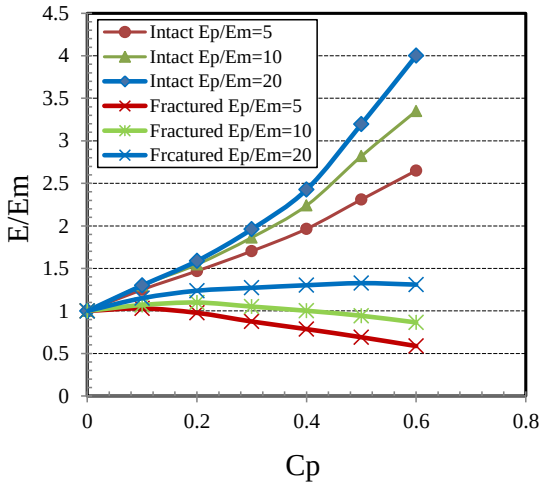

Fig. 6 – Effective stiffness of the composite as a function of particle volume fraction (C_p) for intact and fractured particle

A little increase in the stiffness due to increase the particle's stiffness for the E_p/E_m is witnessed, in comparison to the former case, where E/E_m becomes 1.3-3.25 for the $C_p = 0.1$-0.6 for intact cases. Whereas a reduction of 18 %-75 % noticed for the stiffness for the same range of Cp. More E_p/E_m causes more stiffness levels (i.e., 1.3-4), but for the cracked particle, less impact predicted than the other studied cases (i.e., $E_p/E_m = 5$, 10), but still with high levels of 12 %-68 %.

Figure 7 demonstrates the deformation of RVE which includes a fractured particle, where it is clear that the crack face suffers from axial displacement due to axial load applied.

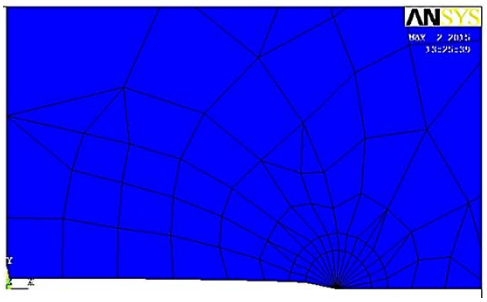

Fig. 7 – Deformed body for the cracked particle of the composite

A clear evidence illustrated from Fig. 8 that stress intensity factor estimated through FEM shows that for $C_p = 10$ %, the normalized levels of SIF starts little bit decreasing for a small crack ($2a/D_p = 1/3$) from 0.73 to 0.67, which is equivalent to 8 % reduction in SIF. This is attributed by the increase of the E_p/E_m to four times than before. As long as the crack length increases, it is anticipated to increase SIF levels, where for fully crack length ($a/D_p = 1/2$), a significant increase in SIF is estimated about 2.5 times at the highest particle stiffness.

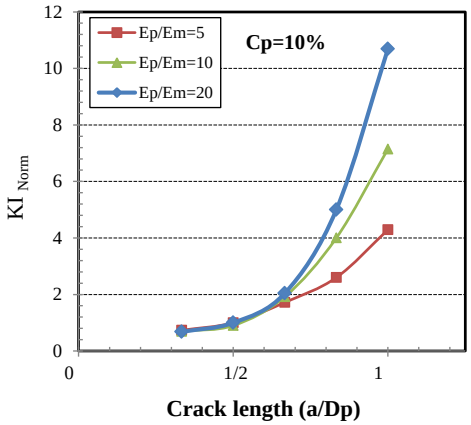

Fig. 8 – Normalized SIF with respect to crack length in fractured particle (C_p = 10 %)

On the other hand, as long as C_p increases for the fractured particle, it is it is observed that KI normalized suffers from reduction in the levels for all E_p/E_m values starting from intact cases up to fully fractures particles. This can be illustrated clearly in Fig. 9.

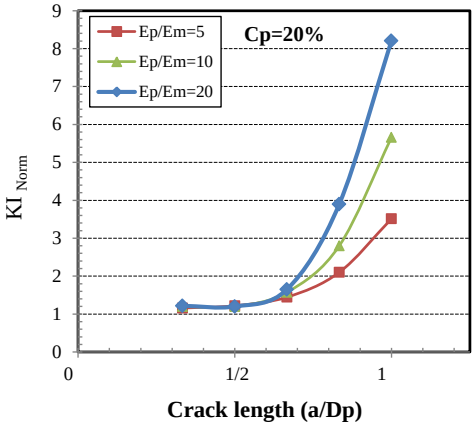

Fig. 9 – Normalized SIF with respect to crack length in fractured particle (Cp = 20 %)

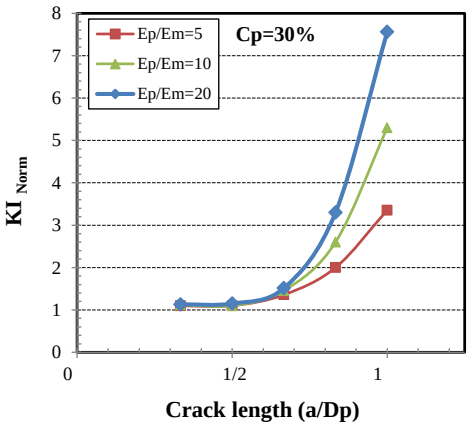

Fig. 10 – Normalized SIF with respect to crack length in fractured particle (C_p = 30 %)

In general, for the C_p = 30 %, a little increase of 3 % in the normalized SIF of the cracked particle is demonstrated in comparison with the previous case for the maximum stiffness ratio adopted in the analysis (i.e. E_p/E_m = 20) and for the shortest crack length of the particle, as shown in Fig. 10. Once the particle considered as fully cracked, a remarkable growth in SIF from 3.4 to 7.6 which is approximated to 124 % increase at the peak particle stiffness.

6. CONCLUSIONS

In general, it has been observed that once the particle becomes deteriorated, a remarkable reduction in the effective stiffness of the composite take place, especially for the fully cracked cases studied. As a consequence, it is expected that this is going to have an impact on the fracture behavior of the particle, where it has been shown that the normalized stress intensity factor of the proposed cracked particle increases as long as the crack length increases. The maximum value occurs when the particle is fully cracked, i.e., the lowest stiffness demonstrated. Beyond this point, the case needs to be more investigated.

REFERENCES

1. O.V. Yushchenko, A.Sh. Baranova, *J. Nano- Electron. Phys.* **2** No 1, 7 (2010).
2. K. Prem Ananth, P. Parasakthi, M. Thiribuvan, K. Prema, R. Karuppaian, N. Sankar, K. Ramachandran, *J. Nano-Electron. Phys.* **3** No 1, 111 (2011).
3. N. Singh, R.M. Mehra, A. Kapoor, *J. Nano- Electron. Phys.* **3** No 1, 132 (2011).
4. S.S. Kanmani, N. Rajkumar, K. Ramachandran, *J. Nano-Electron. Phys.* **3** No 1, 1064 (2011).
5. R. Lydia, P. Sreedhara Reddy, *J. Nano- Electron. Phys.* **5** No 3, 03017 (2013).
6. L. Kozhitov, A. Kuzmenko, D. Muratov, V. Rodionov, A. Popkova, E. Yakushko, M. Dobromyslov, *J. Nano-Electron. Phys.* **6** No 3, 03024 (2014).
7. A.S. Ibraheam, Y. Al-Douri, U. Hashim, M.R. Ghezzarb, A. Addou, Waleed K. Ahmed, *Sol. Energ.* **114**, 39 (2015).
8. M.B. Cil, K.A. Alshibli, *C.R. Mecanique* **343**, 133 (2015).
9. H. Wang, Y. Bai, S. Liu, J. Wu, C.P. Wong, *Acta Materia?-lia* **50** No 17, 4369 (2002).
10. G.M. Asmelash, O. Mamat, *Int. J. Microstruct. Mater. Prop.* **7** No 1, 64 (2012).
11. P. Gurusamy, S.B. Prabu, *Int. J. Microstruct. Mater. Prop.* **8** No 4/5, 299 (2013).
12. H. Teng, *Mechanics Res. Commun.* **52**, 81 (2013).
13. H. Teng, *Finite Elements in Analysis and Design* **65**, 32 (2013).
14. W.K. Ahmed, K. Aslantas, Y. Al-Doury, *J. Nanostruct. Polym. Nanocomposit.* **9** No 3, 59 (2013).
15. T. Mori, K. Tanaka, *Acta Metal.* **21**, 571 (1973).
16. B. Budiansky, R.J. O'Connell, *Int. J. Solid. Struct.* **12** No 2, 81 (1976).
17. Y. Benveniste, *Mechan. Mater.* **6** No 2, 147 (1987).
18. Y. Jiang, H. Yang, W. Guo, *Mater. Sci. Eng.: A* **492** No 1-2, 370 (2008).
19. L. Babout, Y. Brechet, E. Maire, R. Fougeres, *Acta Mater.* **52**, 4517 (2004).
20. L. Mishnaevsky, K. Derrien, D. Baptiste, *Compos. Sci. Technol.* **64** No 12, 1805 (2004).
21. E. Maire, D.S. Wilkinson, J.D. Wilkinson, R. Fougeres, *Acta Mater.* **45** No 12, 5261 (1997).
22. W.K. Ahmed, *J. Nano- Electron. Phys.* **5** No 4, 04059 (2013).
23. L.A. Godoy, V. Mondragón, M.A. Pando, F.J. Acosta, *Int. J. Microstruct. Mater. Prop.* **8** No 3, 185 (2013).
24. X. Liang, H. Li, W. Yu, X. Jiang, Z. Zhang, *ICIC Express Lett.* **6** No 6, 1549 (2012).
25. J.-S. Jang, R.F. Gibson, J. Suhr, *The Int. Soc. Opt. Eng.* **8342**, 83420A (2012).
26. E. Lin, H. Chen, Y. Liu, *Finite Elements in Analysis and Design* **93**, 1 (2015).
27. W.K. Ahmed, S.A. Shakir, *The Int. J. Nanoelectron. Mater.* **7** No 2, 157 (2014).
28. Y. Hua, L. Gu, *Composites Part B: Eng.* **45** No 1, 1464 (2013).
29. N.K. Sharma, S.N. Pandit, R. Vaish, V. Srivastava, *Computational Mater. Sci.* **82**, 320 (2014).
30. V. Kumar, A. Ghosh, *Theoret. Appl. Fracture Mechan.* **75**, 22 (2015).
31. W.K. Ahmed, H. Teng, *Int. J. Microstruct. Mater. Prop.* **9** No 2, 160 (2014).
32. R.Jr. Richards, CRC Press, Boca Raton London New York Washington, D.C. (2001).
33. T. Mochida, M. Taya, D.J. Lloyd, *Mater. Transaction.* **32** No 10, 931 (1991).
34. Y-L. Shen, M. Finot, A. Needleman, S. Suresh, *Acta Metallurgica et Materialia* **42** No 1, 77 (1994).